Bull. Mater. Sci., Vol. 34, No. 2, April 2011, pp. 357–364. © Indian Academy of Sciences.

Synthesis and degradation properties of β-TCP/BG porous composite materials

FAN XIN, CHEN JIAN, RUAN JIANMING*, ZHOU ZHONGCHENG and ZOU JIANPENG
State Key Laboratory of Powder Metallurgy, Central South University, Changsha 410083, People's Republic of China

MS received 16 December 2008

Abstract. **β-TCP/BG porous composite materials were successfully fabricated by foaming technology. X-ray diffraction was used to determine the crystal structure of powders. The pore size and distribution of the resulting materials were characterized using scanning electron microscopy. The porosity and degradation performance of materials were also investigated. The results showed that the porous composite materials possessed the pore size ranging from 100 to 500 μm in diameter, whereas the interconnection among macrospores was poor. The porosity in materials increased from 58·7% to 63·47% with BG content ranging from 0 to 3 wt%, further increasing of BG content results in a decrease in porosity. The degradation rate of composite materials can be adjusted by varying the BG content.**

Keywords. **Composite material; synthesis; performance; porosity; degradation rate.**

1. Introduction

Calcium phosphate-based bioceramics, as artificial materials for bone repair and bone regeneration, have recently received more and more attention due to similar mineral components to those of live bones (Burg *et al* 2000) and excellent biocompatibility and bioactivity (Alam *et al* 2001; Kurashina *et al* 2002; Descamps *et al* 2008). Among the calcium phosphate-based bioceramics, hydroxyapatite [HA, $Ca_{10}(PO_4)_6(OH)_2$] and β-tricalcium phosphate [β-TCP, β-$Ca_3(PO_4)_2$] are probably the most widely studied materials. The rate of degradation of HA is rather too slow after implantation due to its stability in body fluid, whereas that of β-TCP is too fast because of its good solubility and resorbability in body fluid (Daculsi *et al* 1990; Saito *et al* 2000), which limited their wider applications in biomedical fields. Therefore, to obtain the desired rate of degradation after implantation in human body, biphasic calcium phosphate (BCP) composites such as hydroxyapatite–calcium pyrophosphate (HA–CPP) mesoporous bioceramic (Zhao *et al* 2008), HA–TCP material (Ng *et al* 2008), tricalcium phosphate–calcium silicate (Lin *et al* 2006) and tricalcium phosphate–bioactive pyrophosphate glass (Yu *et al* 2008) have been investigated for sick or damaged bone tissues repair and reconstruction in recent years. Moreover, it has been found that the biphasic composites exhibited better bioactive properties and had excellent biodegradability. To the best of our knowledge, no work regarding porous composite materials based on β-TCP and bioactive glass (BG) containing $CaO–P_2O_5–Na_2O–MgO$ have been reported so far.

It is well known that bioactive glass (BG), whose chemical composition is also close to that of the bone mineral phase (Rámila and Vallet-Regí 2001), possesses excellent biocompatibility and osteoconductivity, especially biodegradability and osteoinductivity (Hench *et al* 1971; Roether *et al* 2002; Arinzeh *et al* 2005). Bioactive glass could induce the proliferation and osteogenic differentiation of human osteoblasts by stimulating the progression of osteoblasts (Xynos *et al* 2000). In addition, it shows mechanically direct bonding to living bone tissue after implantation due to the formation of an apatite layer on its surface, facilitating tight fixation of the implants with bone tissue (Arinzeh *et al* 2005). In previous works, we have demonstrated the synthesis of BG by sol–gel method, and the sol–gel processes have the advantages of low reaction temperature and homogenous composition in particles (Zhou *et al* 2008).

For biomaterial ceramics, besides biodegradability and biocompatibility, porosity is another key property. The ideal structures for materials must be formed by an interconnected porous network with a wide variety of pores size, macropores that allow tissue ingrowth and vascularization of the newly formed tissue, and pores in the microporous range to promote protein adhesion and consequently cell adhesion and proliferation. It has been postulated that these micropores concentrate on endogenous bone growth factors on their surfaces through a dissolution–precipitation process (Ripamonti *et al* 1999). These growth factors may induce the differentiation of circulating stem cells into osteoblasts that produce bone tissue. Furthermore,

*Author for correspondence (jianming@mail.csu.edu.cn)

several studies have recently demonstrated that micropores exhibit osteoinductive properties as they are able to form mineralized bone tissue within 6–24 weeks after implantation into the muscles of large animals (Habibovic *et al* 2005; Nihouannen *et al* 2005).

Herein, it is significant and necessary to prepare the composite materials with excellent biodegradable and osteoinductive properties and desired porosity. In the present work, porous composite materials based on β-TCP and BG containing CaO–P_2O_5–Na_2O–MgO (up to 5 wt% according to Santos (Santos *et al* 1994, 1996)) are prepared. The composite materials with varying β-TCP/BG ratios were fabricated by sintering at 1000°C. Fourier transform infrared (FTIR) spectroscopy was used to characterize the chemical composition of BG. X-ray diffraction (XRD) was utilized to examine the crystal structure of samples. The morphology of composite materials was observed using scanning electron microscopy (SEM). The effect of β-TCP/BG ratios on the porosity, and the changes of water absorption as a function of β-TCP/BG ratios as well as degradation time were also investigated.

2. Experimental

2.1 *Materials*

Diammonium phosphate, calcium nitrate tetrahydrate, magnesium nitrate hexahydrate, calcium carbonate, sodium carbonate, and ammonia were purchased from Tianjin Damao Chemical reagent factory. All the chemicals were of analytical grade and were used as received. All the slurries were aqueous, and distilled water was used throughout the experiments.

2.2 *Preparation of β-TCP and BG powders*

β-TCP powder was prepared by chemical precipitation process reported in a previous paper (Liu and Ruan 2004) by adding the solution (0·1 M) composed of diammonium phosphate and calcium nitrate into the calcium nitrate solution (0·1 M) dropwise under vigorous stirring. The corresponding reaction can be described as below:

$$3\mathrm{Ca}\,(\mathrm{NO_3})_2{\cdot}4\mathrm{H_2O} + 2\,(\mathrm{NH_4})_2\,\mathrm{HPO_4} + 2\mathrm{NH_4OH} = \mathrm{Ca_3}\,(\mathrm{PO_4})_2 \downarrow + 6\mathrm{NH_4NO_3} + 14\mathrm{H_2O}. \quad (1)$$

The resulting white precipitate was collected and washed with distilled water and ethanol alternatively, followed by drying at 120°C overnight. β-TCP powder was finally obtained by sintering the dried powder at 1000°C for 8 h.

BG powder composed of CaO–P_2O_5–Na_2O–MgO was synthesized by sol–gel process (Zhou *et al* 2008) using tetraethoxysilane (TEOS), triethylphosphate (TEP), calcium nitrate tetrahydrate, sodium nitrate, magnesium nitrate hexahydrate and ammonia as raw materials. The prepared precursors were heated at 60°C for three days and dried at 160°C for 8 h, then further crushed and ground into powder by ball milling with high density polyethylene (HDPE) milling jar for about 1·5 h. The detailed components of BG are shown in table 1.

Table 1. Component of bioactive glass.

Component	Raw materials	Proportion (wt%)
P_2O_5	$PO(OC_2H_5)_3$	80–78
CaO	$Ca(NO_3)_2{\cdot}4H_2O$	18–16
Na_2O	$NaNO_3$	15–12
MgO	$Mg(NO_3)_2{\cdot}6H_2O$	5–3

2.3 *Fabrication of porous composite materials*

Porous composite materials composed of β-TCP and BG powders were prepared by foaming technology (Vitale-Brovarone *et al* 2007) using spherical polyethylene glycol with a diameter of 300–800 μm as porogen. Briefly, β-TCP and BG powders with various weight ratios were vibrated overnight to homogenize the mixture before adding into the solutions containing spherical polyethylene glycol to form the slurry. The resulting slurry was filtrated and transferred to a high-pressure chamber and compressed at 110 MPa for 10 min, followed by sintering at 1000°C for 8 h in a muffle furnace (Scientific Instrument, China) to fabricate the composite materials. The composite materials containing BG contents of 0, 1, 2, 3, 4 wt% were labelled as (a), (b), (c), (d) and (e), respectively.

2.4 *In vitro degradation*

In vitro degradation of β-TCP/BG porous composite materials was carried out by incubating the samples into phosphate-buffered saline (PBS) at 37·1°C and pH 7·4 under static conditions for 16 days. Detailed descriptions for degradation process are listed in table 2. The incubation medium was replaced by fresh PBS solution everyday. The pH value of the PBS solution during degradation was monitored by a pH meter (Kelong KL-0091 pH meter). Six parallel samples of each degradation conditions were taken out everyday, washed with distilled water and vacuum-dried for further characterizations.

2.5 *Characterization*

2.5a *FTIR*: Chemical structure and chemical composition of BG powder were characterized using Fourier transform infrared (FTIR) spectroscopy (Perkin-Elmer 2000, USA).

Table 2. Degradation condition of β-TCP/BG porous composite scaffolds.

Items	Conditions
Medium	PBS, pH 7·4, 37·1°C
Loading states	Six porous scaffolds were placed in a 50 mL glass bottle containing 24 mL PBS solution. The samples were stored in a shaking water bath with 50 rpm at 37·1±0·1°C for up to 16 days
Dosage of PBS	One scaffolds with 4 mL PBS solution, six scaffolds in one bottle
Interval of PBS changes	At intervals, the pH of the PBS solution was measured and replaced by fresh PBS

2.5b *XRD*: XRD was utilized to characterize the crystal structures of β-TCP powder, BG powder and β-TCP/BG composite materials, using a Philips X'Pert MPD X-ray diffractometer with CuKα ($\lambda = 0{\cdot}15418$ nm) incident radiation.

2.5c *SEM*: The morphology of the materials was observed using scanning electron microscope (SEM, KYKY-2800, China) after gold-coating.

2.5d *Porosity*: Hydrostatic weighing method was used to measure the porosity of composite materials. The porosity was estimated using the formula as follows (Shi *et al* 2001):

$$P_a = (m_3 - m_1)/(m_3 - m_2) \times 100\%, \quad (2)$$

where P_a is the porosity of samples, m_1 the mass of the samples in air before dipping into water (g), m_2 the mass of the samples in water (g), and m_3 the mass of the samples in air after dipping into water (g).

2.5e *Water absorption and mass loss*: Material samples were taken out from the PBS solution at intervals and weighed after wiping off water on the surface to get the wet mass, m_w. Samples were then washed with distilled water and dried in vacuum for 24 h. The dried mass was characterized as m_d. Water absorption of the samples was calculated by the following equation:

$$\text{Water absorption} = (m_w - m_d)/m_d \times 100\% . \quad (3)$$

The original mass of the samples was designated as m_0. Mass loss of the samples (m_{loss}) after degradation for certain time was then calculated as follows:

$$m_{loss} = (m_0 - m_d)/m_0 \times 100\% . \quad (4)$$

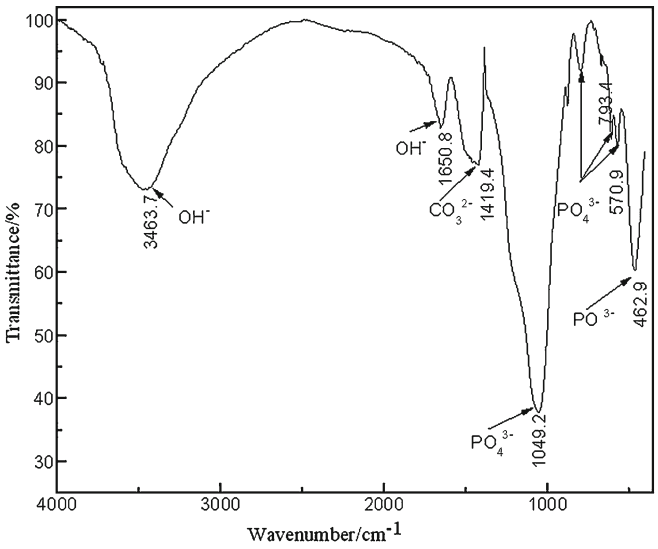

Figure 1. IR spectrum of $CaO–P_2O_5–Na_2O–MgO$ bioactive glass powder.

Table 3. IR vibration modes of $CaO–P_2O_5–Na_2O–MgO$ bioactive glass and pure P_2O_5 glass.

Pure P_2O_5 glass	$CaO–P_2O_5–Na_2O–MgO$ bioactive glass	Vibration modes
500 (S)	462·9 (S)	δ (OPO)
750 (M)	793·4 (M)	ν_s (POP)
1100 (S)	1049·2 (S)	ν_{as} (POP)

Note: S, strong; M, middle; δ, bending vibration; ν_{as}, asymmetric stretching vibration; ν_s, symmetric stretching vibration.

3. Results and discussion

3.1 *FTIR analysis*

The infrared spectrum of BG powder is shown in figure 1. As shown in the spectrum, the absorption bands at 462·9, 570·9, 605·7, 793·4 and 1049·2 cm^{-1} are ascribed to PO_4^{3-} ions. While the band at 1419·4 cm^{-1} is assigned to CO_3^{2-} ions (Manjubala and Sivakumar 2001). Moreover, an absorption band at 3463·7 cm^{-1} appears in the IR spectrum, indicating that a lot of hydroxyl groups still exist on the surface of BG particles, which can provide the active sites for chemical interactions between β-TCP and BG particles to form the strong bonding combination between them. Table 3 illustrates the vibration modes of $CaO–P_2O_5–Na_2O–MgO$ bioactive glass and pure P_2O_5 glass. As can be seen from table 3, the vibration modes of PO_4^{3-} in bioactive glass are similar to those in pure P_2O_5 glass, and both are composed of PO_4 tetrahedral with three-dimensional network structure (Tas 2000).

3.2 *XRD characterization*

The XRD patterns of the received BG, β-TCP and β-TCP/BG powders are shown in figure 2. It can be seen from figure 2(a), that only a broad band exist in the pattern, indicative of the preparation of amorphous BG powder. As illustrated in figure 2(b), all the diffraction peaks are sharp and narrow, which can be perfectly indexed to the crystalline phase of standard β-TCP in the diffraction file (JCPDS No. 09-0169). No peaks indexed to other phases are detected with XRD patterns. All these indicate that β-TCP with perfect crystals can be fabricated by sintering at 1000°C. It has been reported that β-TCP is stable below 1180°C (Ryu *et al* 2002).

According to the Scherrer equation (Fujita *et al* 2000), the average crystallite size of the prepared β-TCP powder is 3·6 μm in diameter. Figure 2(c) shows the XRD pattern of composite materials, indicating that both characteristic peaks corresponding to β-TCP phase and BG phase, respectively are identified. The appearance of diffraction peaks for BG might be due to crystallization reaction when the composite powders were sintered at 1000°C. In other words, small amount of amorphous bioactive glass converted into crystallite-glass. It has been stated that reaction between HA and amorphous glass may occur at sintering temperature, and the final phase transformation may take place (Tancred *et al* 2001).

3.3 *Porosity changes*

In this study, the porosity of composite materials was measured and presented in figure 3. It can be clearly seen that porosity increased first with increasing BG content, and then reached a maximum of 63·47% when the BG content

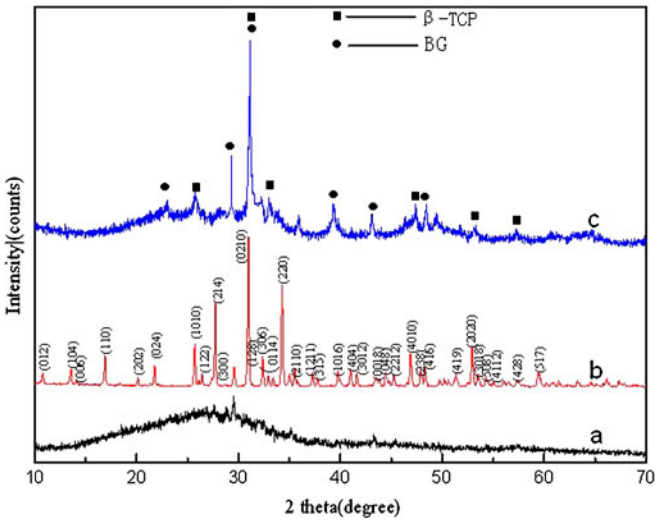

Figure 2. XRD patterns of samples: **a**. BG powder; **b**. β-TCP powder and **c**. β-TCP/BG powder.

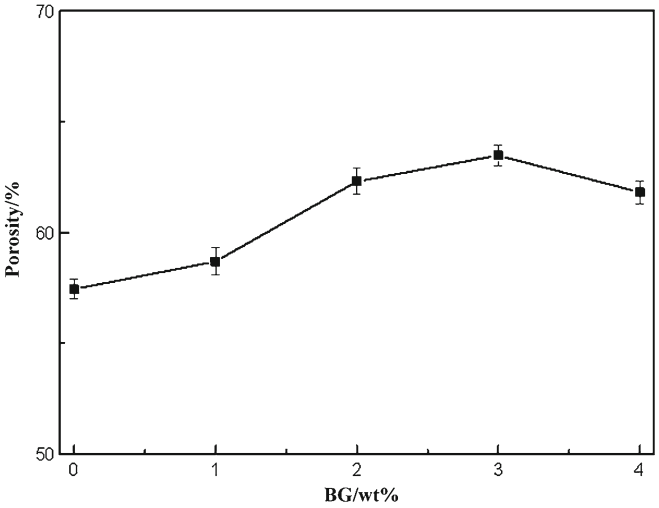

Figure 3. Porosity changes of composite scaffolds with BG content.

was 3 wt%. However, further increasing the amount of BG beyond this level resulted in the decrease of porosity, which may be ascribed to dwindling of pore size and appearance of conglutination phenomena on the material surface.

Highly porous portions allow the ingrowth of bone tissue, while less dense portions allow a load-bearing capacity similar to natural bone. Highly porous structure of composites can provide enormous surface area and pores for cell adhesion, ingrowth, proliferation and differentiation. High porosity (∼50%) is also beneficial for the deposition of extracellular matrix, entrance of nutrients and oxygen and excretion of metabolin (Gauthier *et al* 1999). In this study, the received composite materials possessed the porosity between 58·7% and 63·47%, indicating that the materials can meet the requirement of porosity for biomaterial ceramics and be used as biomedical materials.

3.4 *Morphology*

The morphologies of the obtained composite materials are illustrated in figure 4, indicative of open porous structures for all the samples. SEM image of pure β-TCP powder (figure 4a) shows a large number of particles with uniform pore size forming tight junctions. As illustrated in figures 4(b)–(d), after incorporating BG powder into β-TCP powder, the pore size of composite materials became larger than that of pure β-TCP material. However, while increasing the BG powder to 4 wt%, the pore size of composite materials decreased slightly (figure 4e), revealing the crystallization of amorphous BG powder in composites during sintering at 1000°C. As for the bioceramic materials, the pore size is a key factor for cell growth in pores and on the surface due to convenient entrance of sufficient nutrients and oxygen and metabolism (Fauter *et al* 2001; Ruan and Grant 2001). It has

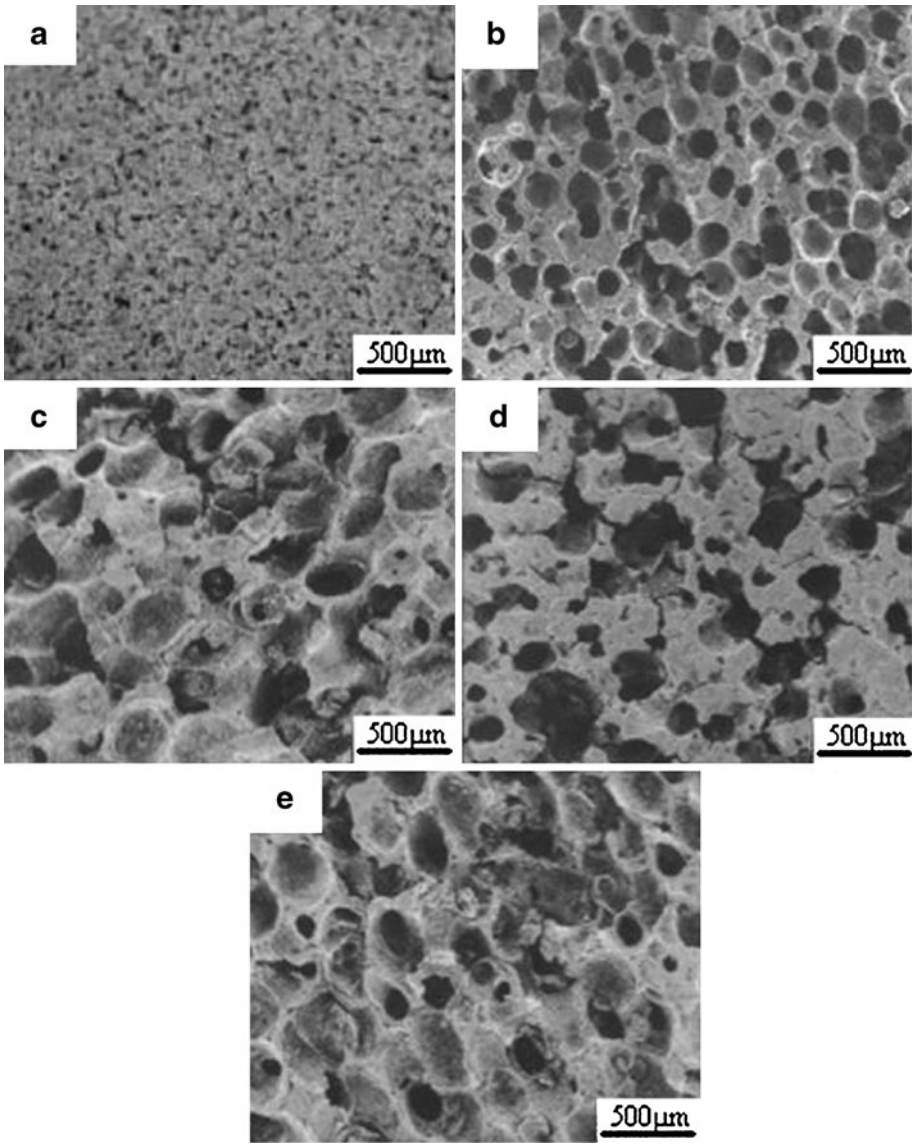

Figure 4. Morphologies of composite scaffolds.

been demonstrated that open pores with pore size ranging from 100 to 800 μm favours body fluid invasion, cell colonization, vascularization and bone tissue ingrowth. Macropores are beneficial to allow cells to move into the pores and cellular metabolism, promoting tissue ingrowth and vascularization of the newly formed tissue. On the other hand, micropores promote protein adhesion and consequently cell adhesion and proliferation, exhibiting osteoinductive performance as they can form mineralization bone tissue within 6–24 weeks after implantation into the muscles of large animals (Habibovic *et al* 2005; Nihouannen *et al* 2005). For bone tissue cell growth in the pores, cell number is enough, because the environmental condition must meet for cell proliferation depending on cell communication with each other. In other words, the proliferation rate increases with increasing the cell density (Jones *et al* 2006). Additionally, the structure of bioceramics also plays an important role in the osteointegration (Gauthier *et al* 1999, 2001). In the present work, we successfully produced the porous composite materials with open macropores and micropores ranging from 100 to 500 μm in diameter (figure 4) and with a porosity between 58·7% and 63·47% (figure 3). However, the macropores of the composite materials were poorly interconnected. The macropores for bone tissue engineering should be interconnected in order to make possible bone healing from the edges towards the centre of the filled defects (Li *et al* 2002) and ensure uniform cell seeding, proliferation and the permeability of the culture medium (Li *et al* 2003). Therefore, the interconnection of macropores is highly relevant for body fluid invasion, colonization of cells, bone ingrowth and vascularization. We have attempted to improve the interconnection of pores by several methods, but fortunately, our

attempts were not successful due to mechanics failure of the materials.

3.5 *pH value*

Figure 5 shows the pH value changes of the PBS solution during degradation of pure β-TCP material and β-TCP/BG porous composite materials. For all the samples, the pH values of PBS increased gradually and reached a certain value with degradation time. From there on until the 16th day, the pH values rapidly decreased. For pure β-TCP material, the pH values reached the maximum quickly at 11th day. In addition, the greater increase in the pH values of PBS occurred from the 4th to the 8th day. Nevertheless, for the composite materials except for that containing BG content of 3 wt%, the pH values of PBS increased slowly than that of pure β-TCP material during incubation for 8 days in PBS.

Due to the relatively slow dissolution rate of alkaline β-TCP and BG in materials at the first stage of incubation, the pH values of PBS increased slightly with degradation time. Meanwhile, the interconnected channels between the pores in materials may be improved owing to the dissolution of alkaline β-TCP and BG in materials, leading to the acceleration of dissolution rate. It can be well explained with respect to great increase in the pH values of PBS after incubation for some days. According to Weng *et al* (1997), the bone-like apatite is difficult to nucleate on the surface if the higher favourable supersaturation is not reached. On the other hand, suitable dissolution and release of calcium and phosphate ions is beneficial for the establishment of bone-like apatite on the surface of materials. Therefore, the dissolution and release of more and more calcium and phosphate ions raised the supersaturation of the PBS solution to the level for apatite to nucleate. However, the initial formation rate of apatite is slow. With the increase in dissolution rate of calcium and phosphate ions from the materials, the calcium and phosphate ion concentrations are more and more high, leading to the possible enhancement of apatite formation. Accordingly, a large amount of calcium and phosphate ions were consumed to form apatite, and the pH values of PBS decreased obviously in this case. The pH values would keep constant, once the equilibrium of dissolution and consumption of calcium and phosphate ions after certain incubation time.

Faster acceleration of pH in PBS after incubation of pure β-TCP material was observed in figure 5 due to faster degradation rate of β-TCP than that of BG (Daculsi *et al* 1990; Saito *et al* 2000). With an increase in the porosity of the composite materials, the pH of PBS increased faster and faster. The higher the porosity, the more solution flows into the pores in the materials, resulting in higher dissolution rate of materials. Therefore, the pH of PBS after incubation of composite-material containing BG content of 3% is higher than that after incubation of pure β-TCP material.

3.6 *Water absorption and mass loss*

Water absorption changes and mass loss of composite materials during degradation in the PBS solution are shown in figures 6 and 7, respectively. Results suggested that the water absorption increased gradually in the early incubation stage and increased rapidly thereafter. In the later stage of incubation, the water absorption increased lightly again. As mentioned in §3·5, bone-like apatite would form on the surface of materials simultaneously during incubation. The water absorption process is a balance between the dissolution inorganic materials and formation of bone-like apatite on the materials surface. Slow dissolution rate of inorganic materials during the initial incubation stage resulted in the gradual increase of water absorption. Thereafter, the sharp increase of water absorption revealed the fast degradation of inorganic

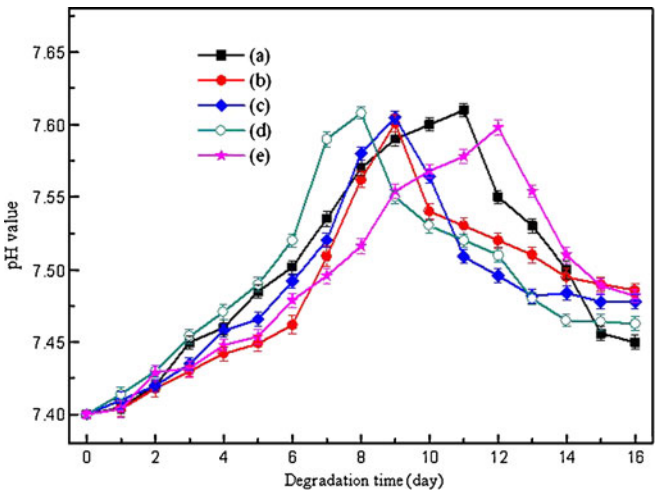

Figure 5. Changes of pH values of PBS solution with degradation time of scaffolds.

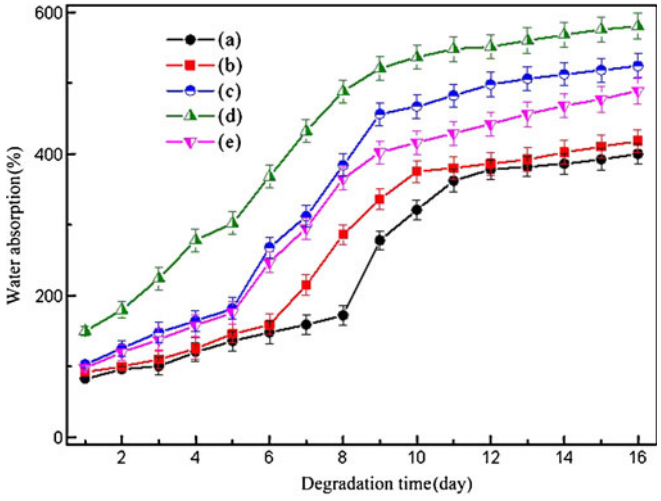

Figure 6. Water absorption changes of scaffolds during degradation.

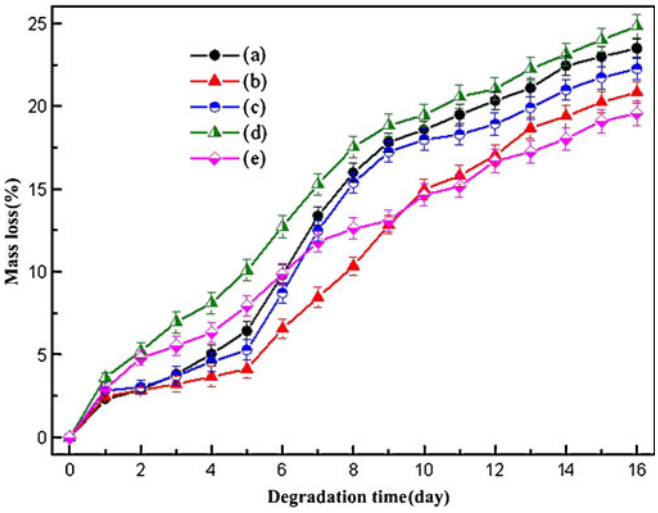

Figure 7. Mass loss of β-TCP/BG composite scaffolds during degradation.

materials in materials. Acceleration of consumption of calcium and phosphate ions due to greater formation rate of apatite led to reduced dissolution rate of material surface, resulting in slight increase of water absorption in the later stage of incubation (Li and Chang 2005).

It can be seen from figure 7 that the degradation rate of pure β-TCP material is faster than that of composite materials. On the other hand, the water absorption in pure β-TCP material is lower than that in composite materials (figure 6) due to its lower porosity and densification (as illustrated in figures 3 and 4(a–d)) although the degradation rate of β-TCP is faster than that of BG. However, when the BG content in composite materials increased up to 4 wt%, the water absorption became lower instead because of poor interconnection between pores in materials (figure 4e).

4. Conclusions

β-TCP/BG porous composite materials were prepared successfully using high-crystallinity β-TCP powder and amorphous BG powder by foaming technology. The resulting porous composite materials possessed pore size ranging from 100 to 500 μm in diameter, and the porosity between 58·7% and 63·47%, but the macropores of the composite materials were poorly interconnected. The degradation behaviour of β-TCP/BG porous materials showed that the composite materials possessed higher porosity and relatively slower degradation rate than pure β-TCP material. Therefore, the porosity and the degradation rate in composite materials can be tailored by varying the BG content in composite materials. In the present work, the prepared β-TCP/BG porous composite material with good degradability and absorbability will be a promising biomaterial for bone repairs and bone replacement in medical applications.

Acknowledgements

We thank the National Natural Science Foundation of China (No. 50774096 and 50604017) and the Postgraduate Education and Innovation Project (No. 1343-74334000011) of Central South University (CSU) for the financial support.

References

Alam I, Asahina I, Ohmamiuda K and Enomoto S 2001 *J. Biomed. Mater. Res.* **A54** 129
Arinzeh T L, Tran T, McAlary J and Daculsi G 2005 *Biomaterials* **26** 3631
Burg K J L, Porter S and Kellam J F 2000 *Biomaterials* **21** 2347
Daculsi G, Passuti N, Martin S, Deudon C, LeGeros R Z and Raher S 1990 *J. Biomed. Mater. Res.* **A24** 379
Descamps M, Duhoo T, Monchau F, Lu J, Hardouin P, Hornez J C and Leriche A 2008 *J. Eur. Ceram. Soc.* **28** 149
Fauter B, Descamps M, Delecourt C, Blary M C and Hardouin P 2001 *J. Mater. Sci.: Mater. Med.* **12** 679
Fujita H, Ido K, Matsuda Y, Iida H, Oka M, Kitamura Y and Nakamura T 2000 *J. Biomed. Mater. Res.* **A49** 273
Gauthier O, Bouler J M, Weiss P, Bosco J, Daculsi G and Aguado E 1999 *J. Biomed. Mater. Res.* **A47** 28
Gauthier O, Goyenvalle E, Bouler J M, Guicheux J, Pilet P, Weiss P and Daculsi G 2001 *J. Mater. Sci. Mater.: Med.* **12** 385
Habibovic P, Yuan H, van der Valk C M, Meijer G, van Blitterswijk C A and de Groot K 2005 *Biomaterials* **26** 3565
Hench L L, Splinter R J, Allen W C and Greenlee T K 1971 *J. Biomed. Mater. Res.* **5** 117
Jones J R, Ehrenfried L M and Hench L L 2006 *Biomaterials* **27** 964
Kurashina K, Kurita H, Wu Q, Otsuka A and Kobayashi H 2002 *Biomaterials* **23** 407
Li H Y and Chang J 2005 *Compos. Sci. Technol.* **65** 2226
Li S H, Wijn J R D, Layrolle P and De Groot K 2002 *J. Biomed. Mater. Res.* **61** 109
Li S H, Wijn J R D, Li J, Layrolle P and De Groot K 2003 *Tissue Eng.* **9** 535
Lin K, Chang J, Lu J, Gao J and Zeng Y 2006 *J. Inorg. Mater.* **21** 1429
Liu B and Ruan J 2004 *J. Inorg. Mater.* **19** 832
Manjubala I and Sivakumar M 2001 *Biomaterials* **71** 272
Ng A M H *et al* 2008 *J. Biomed. Mater. Res.* **A85** 301
Nihouannen D L, Daculsi G, Saffarzadeh A, Gauthier O, Delplace S, Pile P T and Layrolle P 2005 *Bone* **36** 1086
Rámila A and Vallet-Regí M 2001 *Biomaterials* **22** 2301
Ripamonti U, Crooks J and Kirkbride A 1999 *South African J. Sci.* **95** 335
Roether J A, Boccaccinib A R, Hench L L, Maquet V, Gautier S and Jerome R 2002 *Biomaterials* **23** 3871
Ruan J and Grant M H 2001 *J. Cent. South Univ. Technol.* **8** 1
Ryu H S, Youn H J, Hong K S, Chang B S, Lee C K and Chung S S 2002 *Biomaterials* **23** 909
Saito M, Shimizu H, Beppu M and Takagi M 2000 *J. Orthop. Res.* **5** 275
Santos J D, Knowles J C, Reis R L, Reis F J, Monteiro F J and Hastings G W 1994 *Biomaterials* **15** 5

Santos J D, Jha L J and Monteiro F J 1996 *J. Mater. Sci.: Mater. Med.* **7** 181
Shi G, Wang S and Bei J 2001 *J. Funct. Polym.* **14** 7
Tancred D C, Carr A J and McCormack B A O 2001 *J. Mater. Sci.: Mater. Med.* **12** 81
Tas A C 2000 *Biomaterials* **21** 1429
Vitale-Brovarone C, Verné E, Robiglio L, Appendino P, Bassi F, Martinasso G, Muzio G and Canuto R 2007 *Acta Biomater.* **3** 199
Weng J, Liu Q, Wolke J G C, Zhang D and De Groot K 1997 *J. Mater. Sci. Lett.* **16** 335
Xynos I D, Hukkanen M V J, Batten J J, Buttery L D K, Hench L L and Polak J M 2000 *Calcif. Tissue Inter.* **67** 321
Yu X, Cai S, Zhang Z and Xu G 2008 *Mater. Sci. Eng.* **C28** 1138
Zhao H *et al* 2008 *Mater. Chem. Phys.* **111** 265
Zhou Z H, Ruan J M, Zou J P, Zhou Z C and Chen L C 2008 *Trans. Nonferrous Met. Soc. China* **18** 1151